

Angular Signatures of Annihilating Dark Matter in the Cosmic Gamma-Ray Background

A. Cuoco¹, J. Brandbyge¹, S. Hannestad¹, T. Haugbølle^{1,2}, G. Miele^{3,4}

¹*Department of Physics and Astronomy, University of Aarhus,
Ny Munkegade, Bygn. 1520 8000 Aarhus Denmark*

²*Instituto de Física Teórica UAM-CSIC, Universidad Autónoma de Madrid, Cantoblanco, 28049 Madrid, Spain*

³*Università “Federico II”, Dipartimento di Scienze Fisiche, Napoli, Italy & INFN Sezione di Napoli*

⁴*Instituto de Física Corpuscular (CSIC-Universitat de València),
Ed. Institutos de Investigación, Apdo. 22085, E-46071 Valencia, Spain*

(Dated: February 9, 2022)

The extragalactic cosmic gamma-ray background (CGB) is an interesting channel to look for signatures of dark matter annihilation. In particular, besides the imprint in the energy spectrum, peculiar anisotropy patterns are expected compared to the case of a pure astrophysical origin of the CGB. We take into account the uncertainties in the dark matter clustering properties on sub-galactic scales, deriving two possible anisotropy scenarios. A clear dark matter angular signature is achieved when the annihilation signal receives only a *moderate* contribution from sub-galactic clumps and/or cuspy haloes. Experimentally, if galactic foregrounds systematics are efficiently kept under control, the angular differences are detectable with the forthcoming GLAST observatory, provided that the annihilation signal contributes to the CGB for a fraction $\gtrsim 10\text{-}20\%$. If, instead, sub-galactic structures have a more prominent role, the astrophysical and dark matter anisotropies become degenerate, correspondingly diluting the DM signature. As complementary observables we also introduce the cross-correlation between surveys of galaxies and the CGB and the cross-correlation between different energy bands of the CGB and we find that they provide a further sensitive tool to detect the dark matter angular signatures.

PACS numbers: 95.35.+d, 95.85.Pw, 98.70.Vc

I. INTRODUCTION

Astronomical and cosmological observations provide overwhelming evidence for the presence of dark matter (DM) (see e.g. [1] for a review). In particular, the combination of various cosmological data sets provides a precise measurement of the amount of DM in the universe: $\Omega_c h^2 \simeq 0.11$ with a 2σ precision of $\sim 5\%$ in the minimal Λ CDM model [2, 3, 4] and $\sim 20\%$ in more extended models [5].

However, despite the noticeable sensitivity to the cosmological abundance of matter (either dark or baryonic), such measurements only weakly constrain the properties and nature of the particle associated to DM, and very weak limits are available on the DM particle mass m_χ and on its couplings. The simplest DM candidate is the Weakly Interacting Massive Particle (WIMP) which is characterized by having been in thermal equilibrium in the early universe (as opposed to for example the sterile neutrino or super-heavy DM), and having decoupled from equilibrium while non-relativistic. In order to get the correct DM abundance the mass of such a particle cannot be larger than ~ 30 TeV [1, 6]. On the other hand, collider experiments provide a lower bound on the mass of $\sim 50 - 100$ GeV [1], depending on the specific particle candidate. Mass of $\mathcal{O}(\text{GeV})$ are however possible if more exotic candidates are considered [7]. The typical thermally averaged DM annihilation cross section in the WIMP scenario is $\langle\sigma_\chi v\rangle \sim 10^{-26} \text{ cm}^3\text{s}^{-1}$ [1]. However, we stress that if the DM is produced out of equilibrium

in the early universe, no bounds can be given and super-massive, GUT scale, DM particles ($m_\chi \sim 10^{15}$ GeV) and cross sections $\langle\sigma_\chi v\rangle \ll 10^{-26} \text{ cm}^3\text{s}^{-1}$ are in principle possible.

From the point of view of particle physics WIMP candidates are very appealing and emerge naturally in Supersymmetric (SUSY) extensions of the standard model or in the Universal Extra Dimensions (UED) model [1]. The sensitivity of accelerator experiments, notably the Large Hadron Collider, and of direct search experiments are approaching the levels required to test the WIMP hypothesis, and a direct discovery of DM WIMPs could happen in the not so distant future.

DM WIMP candidates have thus typically a large annihilation cross section and pair-annihilate into standard model particles that subsequently decay and shower producing large numbers of photons and neutrinos. Such γ -rays from DM annihilation constitute an ideal target for astronomical searches. Thus, astrophysical and cosmological observations can provide a crucial test, complementary to a direct laboratory detection, in the search for the nature of DM particles. Various astrophysical environments have been discussed in detail as promising sites for observation of DM annihilation, among others the galactic center, satellite dwarf galaxies of the Milky Way and clumps of DM in the Milky Way halo. In the following we will focus instead on the all-sky diffuse signal expected in the extragalactic cosmic gamma-ray background (CGB) [8, 9, 10, 11].

Peculiar spectral and angular features can help in disentangling a signal produced by DM from emission by

“ordinary” astrophysical sources. The spectrum of photons from DM annihilation is in general harder than the spectra arising from normal astrophysical processes and exhibit a pronounced cutoff at an energy near m_χ [8, 9]. The resulting emission thus appear like a “bump” in the background astrophysical energy spectrum in the energy range in which the DM signal gives a relevant contribution. However, although this kind of signature would constitute a strong hint of DM annihilation, astrophysical processes that could mimic such behavior are possible.

Another signature, which has been widely studied, is direct annihilation into a state containing photons, resulting in a line in the background spectrum that would constitute a “smoking gun” signature of DM. However, by construction this process is necessarily loop suppressed and in most models the flux is quite small (see, however, [8] for a more thorough discussion).

Peculiar angular signatures thus offer a complementary signature to exclude the remaining degenerate astrophysical interpretations of a signal. An example is the clumpiness of DM at sub-galactic scales [12, 13, 14, 15] investigated by recent zoomed high-resolution N-body simulations [16, 17]: Clumpiness would result in a population of high galactic latitude extended gamma emitters with a typical annihilating DM gamma spectrum. These kinds of objects could hardly be associated to astrophysical emitters (but see [18]). In these models the size of the clumps is expected to have a characteristic distribution and thus the anisotropy of the integrated signal from all the clumps also exhibits a characteristic behavior [12].

Likewise, the expected angular anisotropies both in the case of an astrophysical and of a DM origin of the CGB can be calculated, and have received increasing attention in the last few years [19, 20, 21, 22, 23]. In the following we will further pursue this issue addressing the differences expected in the two cases and their detectability in the light of the improved statistics that will be available, when the GLAST observatory is launched and start to take data in the near future. We will compare throughout the paper our findings in particular with [20, 22] that deal specifically with anisotropies induced by DM annihilation. Already, there have been claims [10, 24] of a DM signal in the CGB as observed by EGRET (see also [25, 26, 27]), although with the limited EGRET statistics and with the uncertainties in the galactic foregrounds, alternative astrophysical explanations cannot be ruled out. On the other hand, with the improved statistics from GLAST, a proper analysis of the anisotropy properties of the CGB should be able to prove, or disprove, the DM interpretation of features in the CGB spectrum.

Complementary to previous studies we shall employ in the following a parametric approach characterizing the expected CGB signal in terms of a few key parameters, that catch the relevant physical aspects of the problem, and varying them in order to assess the robustness and/or model dependence of the possible signatures. A further advantage of this approach is to make explicit the various assumptions employed throughout on which the final sig-

natures depend. The relevant parameters in the following will be the degree of correlation of the CGB sources with matter and the absolute normalization of the signal, or, equivalently, the expected collected statistics. Further, we will also consider complementary anisotropy observables like the cross-correlation between surveys of galaxies and the CGB and the cross-correlation between different energy bands of the CGB. Together with the auto-correlations of the CGB these represent a set of independent observables that can be jointly employed improving considerably the sensitivity to the DM signal.

The paper is organized as follows: In section II we present a discussion of the horizons within which the CGB signal is expected to come, relevant for the determination of the intensity of the CGB anisotropies itself. In section III we introduce the formalism to derive the CGB anisotropies in terms of the angular power spectrum. In section IV we present a forecast for the expected statistics from GLAST and we discuss the possibility of disentangling the DM annihilation signal from that of astrophysical processes. In sections V and VI we introduce the cross-correlation between the CGB and galaxy surveys and the cross-correlation between different energy bands of the CGB and similarly we discuss the different behavior and sensitivity in the two cases of interest. In section VII we discuss how the previous conclusions apply to different possible scenarios for the CGB and DM properties. In section VIII we summarize and conclude.

II. GAMMA-RAY HORIZONS

The extragalactic cosmic gamma-ray signal can be parameterized as [8, 19]

$$I(E_\gamma, \hat{n}) \propto \int_0^\infty \frac{\rho^\alpha(z, \hat{n}, r(z)) g[E_\gamma(1+z)] e^{-\tau(E_\gamma, z)}}{H(z)(1+z)^3} dz, \quad (1)$$

where $g(E) = dN_\gamma/dE$ is the photon spectrum of the sources, E_γ is the energy we observe today, $\rho(z, \hat{n}, r)$ is the matter density in the direction \hat{n} at a comoving distance r , and the redshift z is used as time variable. In the following we will interchangeably use ρ , or ρ_χ when we want to underline the particle nature of DM. The sources are assumed to be distributed proportional to ρ^α . The Hubble expansion rate is related to its present $z=0$ value H_0 through the matter and the cosmological constant energy densities as $H(z) = H_0 \sqrt{\Omega_M(1+z)^3 + \Omega_\Lambda}$, and the reduced Hubble expansion rate $h(z)$ is given by $H(z) = 100 h(z)$ km/s/Mpc. We will in the following use the parameters of the standard Λ CDM model [3], i.e. $\Omega_M = 0.3$, $\Omega_\Lambda = 0.7$ and $H_0 = 70$ km/s/Mpc. The quantity $\tau(E_\gamma, z)$ is the optical depth of photons to absorptions via pair production (PP) on the Extra-galactic Background Light (EBL). In ref. [19] an energy threshold of $E_{\text{cut}} = 100$ GeV has been considered resulting in a PP horizon of about $z \approx 0.5$, and a simple extrapolation back in time of the present EBL gave a sufficiently accurate

value of τ . In the present work we also consider $E_{\text{cut}} = 10$ GeV and horizons as large as $z \approx 4 - 5$. In this range the dynamical evolution of the EBL during the photon propagation becomes important for a correct estimate of τ . To take this into account we use the parametrization of $\tau(E_\gamma, z)$ from [28] for $0 < z < 5$, where evolution effects are included in the calculation. The EBL is expected to be negligible at redshifts higher than $z \approx 5$ corresponding to the peak of star formation. Thus, gamma photons produced at earlier times experience an undisturbed propagation until $z \approx 5$, while only in the recent epoch they start to loose energy, due to scattering on the EBL. Correspondingly, we assume $\tau(E_\gamma, z) = \tau(E_\gamma, 5)$ for $z > 5$ (see also formula (A.6) in [19]).

The case $\alpha = 1$ is generally representative of astrophysical sources following the Large Scale Structure (LSS) of matter, while the case $\alpha = 2$ is appropriate for annihilating DM whose signal follows the square of the matter density, $\propto \rho_\chi^2$ through

$$I_\chi = \frac{\langle \sigma_\chi v \rangle}{8\pi m_\chi^2} \int_0^\infty z \frac{\rho_\chi^2(z, \hat{n}, r(z)) g[E_\gamma(1+z)] e^{-\tau(E_\gamma, z)}}{H(z) (1+z)^3} dz. \quad (2)$$

This last point is however entangled with the exact small scale (sub-galactic) clustering properties of DM and deserves further discussions. If DM clumps on sub-galactic scales, as suggested by various numerical models of galaxy formation, or if the DM halo has a very pronounced spike at its center, the galactic DM signal can be greatly enhanced and the overall cosmological contribution of DM to the CGB would be due to the emission from single galaxies. The $\rho_\chi^2(\vec{x})$ field in Eq.(2) would look approximately as a sum of delta functions centered on the galaxies' positions and the DM annihilation signal would thus trace the matter distribution linearly, (actually, the galaxy distribution), at least at scales larger than the galactic haloes. In this case, however, the DM signal expected from the Milky Way itself would probably be a more promising observable for signatures of DM annihilation, as we will further discuss later. The relative contribution of the galactic versus extra-galactic DM signal is further discussed in [29]. In principle, if the DM clustering properties would be known in the whole range from sub-galactic to cosmological scales, the ratio of the linear to quadratic contribution can be calculated. However, given the still persisting uncertainty in the sub-galactic clumping, to be general we will assume a DM annihilation anisotropy signal $\delta I_\chi / I_\chi \propto \rho_\chi^2 / \bar{\rho}_\chi^2 + \xi \rho_\chi / \bar{\rho}_\chi$, where ξ parameterizes the relative weights of the linear and quadratic contributions. In the following we will discuss mainly the extreme scenarios $\xi \ll 1$ and $\xi \gg 1$ in which one of the two contributions dominates over the other. More precisely, we thus define a ‘‘quadratic scenario’’ in which DM clustering is relevant only above the scale of galactic haloes ($\sim 10^{12} M_\odot$), and a ‘‘linear scenario’’ in which sub-galactic structures dominate the cosmological DM annihilation signal. The mixed scenario is discussed further in section VII.

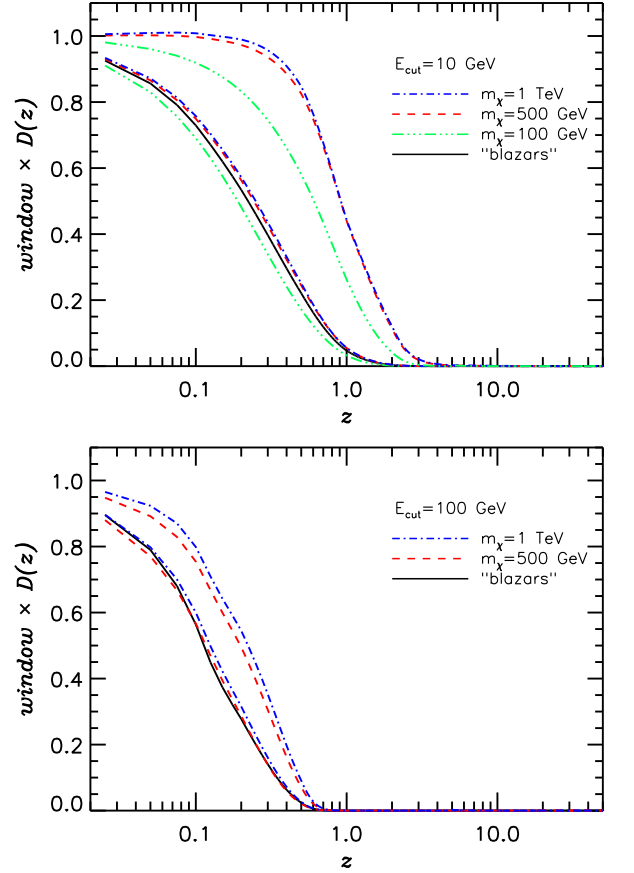


FIG. 1: Gamma window functions times the linear growth factor $D(z)$ for $E_{\text{cut}} = 10, 100$ GeV and for various DM masses. The curves are normalized to 1 at $z = 0$. Upper and lower curves in each panel refer to the DM annihilation signal correlating quadratically and linearly ($\alpha = 2, 1$), respectively, with matter.

The astrophysical and DM window functions, $W_\gamma(E_{\gamma\text{cut}}, z)$ and $W_\chi(E_{\chi\text{cut}}, z)$, which contain the information about gamma-ray propagation, injection spectra and cosmological effects, are defined from Eq. (1) as

$$I_\gamma(E_{\gamma\text{cut}}, \hat{n}) \propto \int_0^\infty z W_\gamma(E_{\gamma\text{cut}}, z) \rho(z, \hat{n}), \quad (3)$$

$$I_\chi(E_{\chi\text{cut}}, \hat{n}) \propto \int_0^\infty z W_\chi(E_{\chi\text{cut}}, z) \rho^2(z, \hat{n}), \quad (4)$$

where we are using the notation $\rho(z, \hat{n}, r(z)) = (1+z)^3 \times \rho(z, \hat{n})$ to underline that the window function is only dependent on the two variables, direction and redshift, and to make explicit the $(1+z)^3$ behavior of the matter density. In principle ρ_s , the density distribution of astrophysical sources, should be used in Eq. (3): ρ_s in general exhibits a scale and time dependent bias with respect to the matter density. However, specific classes of astrophysical gamma-ray sources have different biases. Blazars, for example, that most likely produce the bulk of the CGB signal detected by EGRET, are well known to concentrate at the center of clusters of galaxies, thus

presenting an over-bias with respect to galaxies at high densities. On the other hand, galaxies and clusters of galaxies quite fairly trace the matter density, at least in the recent cosmic epoch. The assumption $\rho_s = \rho$ for I_γ is thus general enough to reasonably describe emission from astrophysical sources.

The window functions can be found from Eq. (1) and are given by

$$W(E_{\text{cut}}, z) \equiv \int_{E_{\text{cut}}}^{\infty} \frac{g[E(1+z)] (1+z)^{3\alpha-3}}{H(z)} e^{-\tau(E,z)}, \quad (5)$$

where $\alpha = 1, 2$ applies in the astrophysical and DM cases, respectively. When properly normalized $W(E_{\text{cut}}, z)$ represents the probability of receiving a photon of $E_\gamma > E_{\text{cut}}$ emitted at a redshift z . It can be used to define an effective horizon, $z_{\mathcal{H}}$, beyond which the probability of receiving a photon is negligible (e.g. $\lesssim 1\%$). For $E_{\text{cut}} \gtrsim 100$ GeV PP losses dominate and the horizon is $z_{\mathcal{H}} \lesssim 1$ independent of the value of α or the shape of $g(E)$. For $E_{\text{cut}} \lesssim 10$ GeV, instead, PP losses start to become negligible ($\tau \approx 0$) and photons propagate freely from arbitrary high redshifts. However, even in this case a horizon exists due to redshifting related this time to the exact shape of the injection spectrum $g(E)$ and the value of α . In the case of astrophysical sources we take $g(E) \propto E^{-2}$, consistent with the observed EGRET CGB spectrum and with the observed spectra of common astrophysical gamma sources like blazars. We found however that for $E_{\text{cut}} = 10$ GeV the horizon is still mainly settled by the cosmological and PP attenuation effects while the exact shape of the spectrum plays a minor role and even choices like $g(E) \propto E^{-1}$ or $g(E) \propto E^{-3}$ change only slightly the astrophysical window. Given the poor sensitivity to the specific details of the emission spectrum we will thus often refer in the following to the term “*blazars*”, meaning in general a representative class of astrophysical gamma-emitters tracing linearly the matter density and with a power law E^{-2} spectrum. The resulting horizon is $z_{\mathcal{H}} \approx 1$ as shown in Fig. 1. The windows are further multiplied by the linear growth factor $D(z)$ that takes into account the evolution of matter clustering in the past (see the next section). $D(z)$ gives a further, although not crucial, contribution to the determination of the exact horizon $z_{\mathcal{H}}$. For $E_{\text{cut}} = 100$ GeV the horizon is instead $z_{\mathcal{H}} \approx 0.5$ and depends exclusively on the EBL absorption both in the astrophysical and DM cases. This makes this energy range particularly interesting due to its limited sensitivity to any particular modelling. Some further effects can in fact contribute to modify the horizon: The luminosity of blazars for example can in principle change with time due to well known source evolution effects introducing a further $(1+z)^\lambda$ factor in the window. While evolution effects are unimportant for $E_{\text{cut}} = 100$ GeV, a strong source evolution can in principle affect $z_{\mathcal{H}}$ at $E_{\text{cut}} = 10$ GeV.

In the case of DM, the spectrum $g(E)$ and the cosmological factors involved are quite different and the effective horizon can be much larger. The different expected

horizon is in fact an important ingredient for a clear discrimination through the expected pattern and intensity of the anisotropies. A commonly used parametrization for the annihilation spectrum of DM is [9]

$$g(E) \propto \frac{\exp(-7.76E/M_\chi)}{(E/M_\chi)^{1.5} + 0.00014}, \quad (6)$$

i.e. a spectrum that is generally harder than the astrophysical E^{-2} spectrum, and with a cutoff near the DM mass energy (that is the behavior responsible for the bump in the overall spectrum). The shape given by Eq. (6) is almost independent of the details of the annihilation process, at least for the case of SUSY WIMPs where the main contribution comes from decays to $q\bar{q}$, ZZ , and W^+W^- , with subsequent hadronization. A slightly different spectrum is expected for the case of decay into a lepton-anti-lepton pair or for the annihilation of UED WIMPs (see [1] for details). We will not further consider these cases although basically our findings also apply to them. The resulting windows depend on the assumed DM mass, m_χ , and on the chosen E_{cut} . Various cases used in the following are shown in Fig. 1. At energies above $E \gtrsim 100$ GeV the photon absorption dominates and, as discussed above, the DM and astrophysical horizons are almost identical, $z_{\mathcal{H}} \approx 0.5$. For $E_{\text{cut}} = 10$ GeV the horizon for astrophysical sources is $z_{\mathcal{H}} \simeq 1$, while that of DM is generally of order $z_{\mathcal{H}} \simeq 3-4$. Very interestingly, we can see that the role of absorption by the EBL is still quite relevant for DMA at $E_{\text{cut}} = 10$ GeV limiting the horizon which otherwise would exceed $z \simeq 10$ giving much smaller DM anisotropies. Finally, for the case of the DM signal correlating linearly with matter ($\alpha = 1$), no appreciable differences are present in the windows neither at the high nor at the low energy cut. Even if the DM spectral shape is quite peculiar, not unexpectedly this seems to play a minor role, as in the previously discussed case of astrophysical emission. In this case the DM and astrophysical signal have degenerate anisotropy properties and this observable cannot further help in disentangling the two contributions.

III. CGB ANISOTROPIES

A. 3D Power Spectra

To derive the CGB anisotropies we need first to know the spatial clustering properties of the matter field ρ and of its square. To this purpose we use a template of the matter distribution derived from a DM N-body simulation.

The N-body simulation was performed with the publicly available code GADGET-2 [30] with 512^3 CDM particles in a $128 \text{ Mpc}/h$ box. We have assumed a flat Λ CDM-model, with $\Omega_{\text{CDM}} = 0.30$, $\Omega_\Lambda = 0.70$ and $h = 0.70$ as well as a scale-invariant primordial power spectrum, $P \propto k$. The transfer function was generated using CMBFAST [31], and then the initial conditions were computed

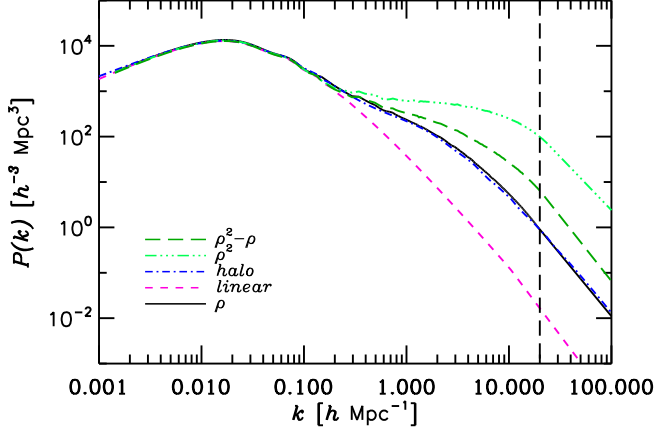


FIG. 2: 3D power spectra of the matter density distribution and of its square, as derived from a cosmological N-body simulation. Also shown is the linear matter power spectrum, the non-linear Halo-model prediction and the cross-correlation between the matter distribution and its square. The vertical dashed line mark the confidence limit on the calculation of $P(k)$. All the spectra are normalized at the linear scales to the matter power spectrum.

using second order Lagrangian perturbation theory [32]. The smoothed density field is constructed by interpolating the particles to a 2048^3 grid, enforcing mass conservation, and using the adaptive spline kernel from [33].

If $\rho(\vec{x})$ denotes the simulation density field and $\rho(\vec{k})$ its Fourier transform, then the matter power spectrum can be written as

$$P_\rho(k) = \int_{S_{\Delta k}} d^3\vec{k} \left| \rho^*(\vec{k}) \rho(\vec{k}) \right|, \quad (7)$$

and analogously

$$P_{\rho^2}(k) = \int_{S_{\Delta k}} d^3\vec{k} \left| \rho_2^*(\vec{k}) \rho_2(\vec{k}) \right|, \quad (8)$$

where $\rho_2(\vec{k})$ denotes the Fourier transform of the *squared* density field $\rho^2(\vec{x})$ and $S_{\Delta k}$ is a spherical shell of radius k and thickness Δk . Finally, it is also possible to estimate the cross-correlation spectrum

$$P_{\rho\rho^2}(k) = \int_{S_{\Delta k}} d^3\vec{k} \left| \rho_2^*(\vec{k}) \rho(\vec{k}) \right|. \quad (9)$$

We take into account the time dependence of $P_i(k, z)$ ($i = \rho, \rho^2, \rho\rho^2$) using the linear growth factor $D(z)$

$$P_i(k, z) = P_i(k, z=0) \times D^2(z), \quad (10)$$

with $D(z) \propto h(z) \int_z^\infty dz' (1+z')/h^3(z')$ and $D(0) = 1$.¹

¹ $D(z)$ is a good approximation also at non-linear scales where $P(k, z)$ grows only slightly faster than the linear growth [34].

In Fig. 2 the various spectra are shown. Notice the increase in power at small scales for $P_{\rho^2}(k)$ compared to $P_\rho(k)$. For reference $P_\rho(k)$ as calculated in the Halo-model [35] is also shown. It can be seen that the spectra from the N-body simulation and the Halo-model are in quite good agreement. However, the N-body spectrum starts to be affected by numerical noise beyond $k \simeq 20 h \text{ Mpc}^{-1}$, shown as a vertical line in the plot, and this range is accordingly excluded from the analysis. The contribution from higher wave numbers, $k \gtrsim 20 h \text{ Mpc}^{-1}$, or, equivalently, smaller scales, $\lambda \lesssim 2\pi/20 h^{-1} \text{ Mpc}$, is in any case relevant only for very high multipoles $l \gtrsim 1000$ not accessible experimentally, so that for the present purposes they can be safely neglected. The spectrum of the squared matter distribution is also in fair agreement with the Halo-model calculation as derived in [20]. The most noticeable feature is an increase in the intensity of the anisotropies at the non-linear scales $k \gtrsim 1.0 h \text{ Mpc}^{-1}$ with respect to the matter spectrum, understandable in the framework of the Halo-model as a dominant contribution from the single-halo term. As expected the cross-correlation is in between the matter and the matter squared spectra. In the figure all the spectra are normalized to the matter spectrum at linear scales, while the absolute normalization for the matter squared and for the cross-correlation is given by 4 and 2 times this value, respectively.

B. Angular anisotropies

From Eq.(3)-(4) we can now easily construct the angular power spectra of the various dimensionless fluctuation fields $\delta I/I$

$$C_\gamma^l = \int \frac{dr}{r^2} W_\gamma^2(r) P_\rho \left(k = \frac{l}{r}, z(r) \right), \quad (11)$$

$$C_{\chi 1}^l = \int \frac{dr}{r^2} W_{\chi 1}^2(r) P_\rho \left(k = \frac{l}{r}, z(r) \right), \quad (12)$$

$$C_{\chi 2}^l = \int \frac{dr}{r^2} W_{\chi 2}^2(r) P_{\rho^2} \left(k = \frac{l}{r}, z(r) \right), \quad (13)$$

for the astrophysical and DM cases following linearly or quadratically the matter distribution, respectively.² We have used the Limber approximation, which is accurate for all but the very lowest multipoles.

In principle the intermediate case of a DM signal $\propto \rho_\chi^2/\bar{\rho}_\chi^2 + \xi \rho_\chi/\bar{\rho}_\chi$ can also easily be derived, giving a final spectrum

$$C_\chi^l = \frac{1}{(1+\xi)^2} C_{\chi 1}^l + \frac{\xi^2}{(1+\xi)^2} C_{\chi 2}^l + \frac{2\xi}{(1+\xi)^2} C_{\chi 12}^l, \quad (14)$$

² The angular spectra calculations involve an integral over r , the comoving distance, while the windows are known in terms of the redshift z . We thus use the r - z relation $r(z) = c/H_0 \int_0^z dz' 1/\sqrt{\Omega_m(1+z')^3 + \Omega_\Lambda}$, and its inverse $z(r)$.

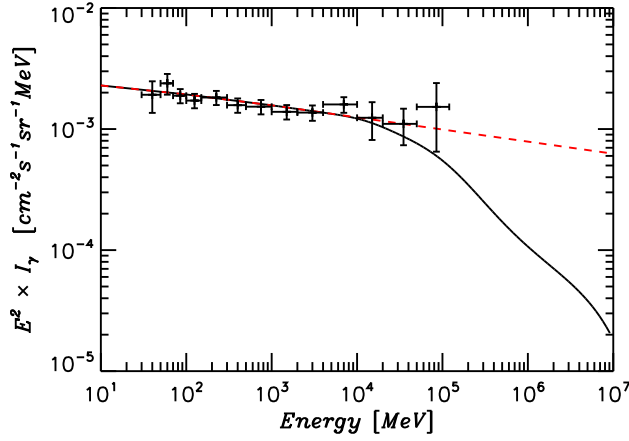


FIG. 3: EGRET spectrum from [36] and extrapolation up to 10 TeV. The solid line shows the expected effect of the PP attenuation.

where the $\rho\text{-}\rho^2$ spectrum is involved

$$C_{\chi 12}^l = \int \frac{dr}{r^2} W_{\chi 1}(r) W_{\chi 2}(r) P_{\rho\rho^2} \left(k = \frac{l}{r}, z(r) \right), \quad (15)$$

and $0 \leq \xi \leq \infty$ weights the relative contribution of the linear and quadratic correlation terms. In practice, however, in the following we will mainly consider the two cases $\xi = 0, \infty$, while the intermediate case is easily understandable with a qualitative discussion. We will however consider quantitatively a mixed scenario in section VII.

IV. CGB AUTO-CORRELATION ANALYSIS

A. Forecast assumptions and sensitivity

In this section we describe our assumptions to assess the sensitivity of the forthcoming gamma-ray detectors, in particular GLAST, to the angular signatures in the auto-correlation spectrum described in the previous section. Similarly, the sensitivity of the cross-correlation observables is discussed in the next sections.

The observed diffuse gamma emission is constituted by the sum of the CGB and of the diffuse galactic emission, so that, experimentally, the relevant extragalactic signal needs to be separated from the related galactic foregrounds. We will assume in the following a perfect removal of the galactic gamma foregrounds from the CGB. We will thus quote statistical errors only. Indeed, foreground separation will be a non trivial issue in the analysis of the forthcoming datasets and this is turn is expected to propagate to the determination of the CGB anisotropies. A detailed analysis of the effects of the foregrounds is beyond the scope of this work. We will however further discuss this point in section VII.

We consider the diffuse energy spectrum as measured by EGRET [36]

$$I(E_\gamma) = k_0 \left(\frac{E}{0.451 \text{ GeV}} \right)^{-2.10 \pm 0.03}, \quad (16)$$

valid from $E \sim 10$ MeV to $E \sim 100$ GeV, where $k_0 = (7.32 \pm 0.34) \times 10^{-6} \text{ cm}^{-2} \text{ s}^{-1} \text{ sr}^{-1} \text{ GeV}^{-1}$, correcting it by the effects of EBL absorption as described in section II. We show in Fig. 3 a plot of the EGRET data [36] together with the fit in Eq. (16) and its extrapolation in the case of PP absorption. In agreement with the result of section II it can be seen again that ~ 10 GeV is the critical energy above which the EBL absorption effects become relevant.

It is then possible to estimate the number of events, N_γ , in the relevant energy range to be collected during the time t as

$$N_\gamma = t \cdot DC \cdot \Omega_{\text{fov}} \cdot \int_{E_{\text{cut}1}}^{E_{\text{cut}2}} dE A_{\text{eff}}(E) I_\gamma(E), \quad (17)$$

where DC is the duty-cycle of the instrument, Ω_{fov} is the solid angle of the field of view and $A_{\text{eff}}(E)$ is the effective collecting area of the instrument (averaged over the field of view of the instrument). For GLAST [37] we will assume a constant $A_{\text{eff}}(E) = 10^4 \text{ cm}^2$, $DC = 90\%$, $\Omega_{\text{fov}} = 2.4 \text{ sr}$ and $f_{\text{fov}} = \Omega_{\text{fov}}/4\pi$. In addition, we use the angular resolution of the experiment ($\sigma_b = 0.115^\circ$) and the associated angular window function $W_l = \exp(-l^2 \sigma_b^2/2)$.

Analogously, the number of photons expected from DM annihilation is given by

$$N_\chi = t \cdot DC \cdot \Omega_{\text{fov}} \cdot \int_{E_{\text{cut}1}}^{E_{\text{cut}2}} dE A_{\text{eff}}(E) I_\chi(E), \quad (18)$$

where $I_\chi(E)$ is the DM annihilation spectrum. In our parametric approach we calculate the statistics N_χ normalizing the DM spectrum to the EGRET spectrum so that $N_\gamma = N_\chi$ for the relevant energy cut. Later we will discuss briefly how the conclusions are affected in the case in which the DM signal is reduced to the 20% of the EGRET value or in the case in which the CGB itself is reduced if parts of it are resolved as sources by GLAST.

The forecasted error bars on the various CGB angular auto-correlation spectra are given by

$$\frac{\delta C_\gamma^l}{C_\gamma^l} = \sqrt{\frac{2(1 + C_{N,\gamma}/W_l^2 C_\gamma^l)^2}{(2l+1)\Delta l f_{\text{fov}}}}, \quad (19)$$

$$\frac{\delta C_\chi^l}{C_\chi^l} = \sqrt{\frac{2(1 + C_{N,\chi}/W_l^2 C_\chi^l)^2}{(2l+1)\Delta l f_{\text{fov}}}}, \quad (20)$$

where $C_{N,\gamma} = \Omega_{\text{fov}}/N_\gamma$ and $C_{N,\chi} = \Omega_{\text{fov}}/N_\chi$ are the gamma and DM random noise levels respectively.

The resulting spectra and their error bars are shown in Fig. 4 for the case of the pure quadratic scenario. In the case of $E_{\text{cut}} = 10$ GeV DM masses of 100, 500 GeV are shown, while for $E_{\text{cut}} = 100$ GeV we consider only

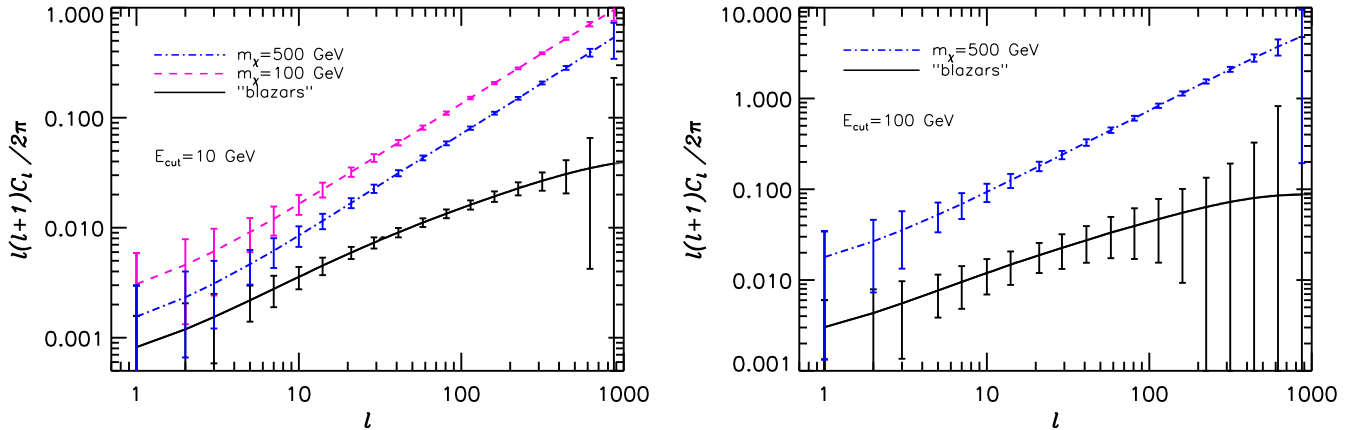


FIG. 4: Angular spectra for $E_{\text{cut}} = 10, 100$ GeV with 1σ error bars for a 4-year GLAST survey.

the value 500 GeV, a mass of 1 TeV showing basically the same spectrum and error bars.

The plot on the right ($E_{\text{cut}} = 100$ GeV) shows quantitatively what was anticipated in the previous section. The windows are almost identical for the DM and the astrophysical cases and the higher intrinsic level of fluctuations of DM produces a much higher normalization in the angular power spectrum. For reasonable values of the DM mass the change in the level of anisotropies is thus measurable and distinguishable from the astrophysical case and provides an important signature of DM emission. Further, the shapes of the angular spectra are quite different, the DM case giving a further enhancement of the fluctuations at small scales $l \gtrsim 100$ as previously found also in [19] (see in particular Fig. 2). The statistics collected above 100 GeV by GLAST in a 4 year period ($N_\gamma \approx 10^4$) is still high enough to allow a more than satisfactory measurement and separation of the various power spectra.

In the $E_{\text{cut}} = 10$ GeV case there is instead a competition between the enhanced level of fluctuations and their dilution in the wider horizon related to DM. The final normalization of the C_l 's is still greater though, than that of blazars although the difference is reduced with respect to $E_{\text{cut}} = 100$ GeV. The increased statistics at low energy and, more importantly, the different shapes of the spectra, however, still make the two contributions separable. For $E_{\text{cut}} = 100$ GeV, relevant in the case of a not too light DM particle $m_\chi \gtrsim 300$ GeV, we further see that the angular spectrum maintains its diagnostic power with the additional advantage that the small horizon involved, $z_H \approx 0.5$, considerably reduces the model dependence of the signature from cosmological evolution or bias effects.

Finally, an important point to consider is that the astrophysical sources' power spectrum, being almost independent of the energy cut, can be measured at low energies, where the collected statistics is high and thus the statistical errors are correspondingly small. This calibra-

tion of the astrophysical signal at low energies can further improve the separation of the two signals especially in the case where the DM flux is not at the EGRET level but significantly below the CGB flux. The amount of separation can be quantified by considering the *cross-correlation* between different energy bins. We will further discuss this point in section VI.

B. Comparison with previous works

The above results for $E_{\text{cut}} = 10$ GeV are in general in good agreement with [20, 22], confirming the sensitivity of the auto-correlation spectrum to the DM signal. In particular we confirm that apart the normalization, the blazar and DM spectra have a quite different shape with the DM case giving much more power to the small scales, i.e. for multipoles $l \gtrsim 100$.

In the present work, with respect to [20] we consider in much more detail the role of photon absorption showing that it is quite relevant also for an energy cut as low as 10 GeV. We have indeed also improved the treatment of the photon absorption process considering the most updated results from [28].

To compare directly our results with that of [20] it should be taken into account that our quadratic model shown in Fig. 4 consider the contribution to anisotropies from haloes greater than average galactic haloes, with a typical mass of $10^{12} M_\odot$. Ref. [20], instead, consider two particular fiducial models with DM clustering until a sub-halo mass scale of $10^6 M_\odot$ and $10^{-6} M_\odot$. Both their model thus consider a certain sub-galactic contribution and can be approximately compared to our mixed scenario (see section VII) with a particular value of the mixing parameter ξ . As expected, indeed, the anisotropy spectra in [20] has a lower normalization corresponding to the fact the DM “linear” contribution tends to drag the fluctuations to the level of the astrophysical ones. A further part of the difference could also arise from our

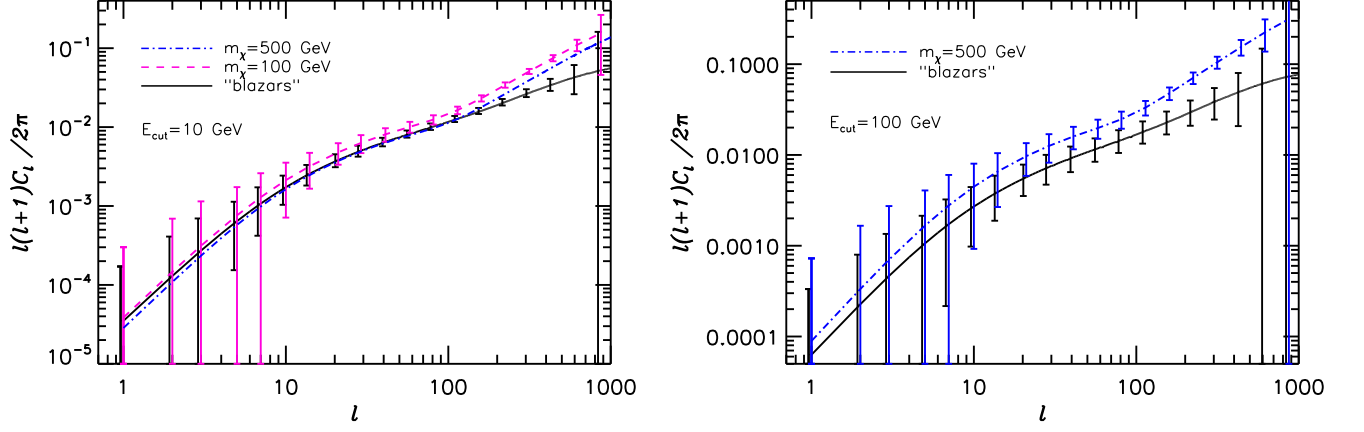


FIG. 5: Angular cross-correlation spectra between the CGB and an example survey of galaxies for $E_{\text{cut}} = 10$ and 100 GeV. Error bars are for a 4-year GLAST survey.

improved treatment of the photon absorption although in this case, as explained above, a direct comparison is difficult.

V. GALAXY-CGB CROSS-CORRELATION

Another observable sensitive to the DM properties can be obtained by looking at the cross-correlation between the CGB and galaxy catalogues. If the CGB is cosmological in origin, clearly a positive cross-correlation is expected. Comparing the cross-correlation originating from DM annihilation to that of astrophysical emission differences are expected, similar to those of the auto-correlation spectrum studied in the previous sections. The same formalism can be generalized to address these differences in detail as we show in the following. Intuitively, the use of the cross-correlation spectrum is a way to go beyond the level of the statistical information only and the limits imposed by cosmic variance exploiting not only the statistical spectrum C_l but also the information contained in the whole sky distribution in terms of the a_{lm} harmonic coefficients [19].

Similarly to the CGB we introduce the galaxy intensity map of the catalogue

$$I_g(\hat{n}) = \int_0^\infty z \frac{dn}{dz}(z) \rho_g(z, \hat{n}), \quad (21)$$

where the galaxy window $W_g(z) = dn/dz(z)$ is in this

case the redshift distribution of the catalogue's galaxies. The related observables in this case are the cross-correlation between gamma emission and galaxies and the DM-galaxy cross-correlation

$$C_{\gamma g}^l = \int \frac{dr}{r^2} W_\gamma(r) W_g(r) P_\rho \left(k = \frac{l}{r}, z(r) \right), \quad (22)$$

$$C_{\chi 1g}^l = \int \frac{dr}{r^2} W_{\chi 1}(r) W_g(r) P_\rho \left(k = \frac{l}{r}, z(r) \right), \quad (23)$$

$$C_{\chi 2g}^l = \int \frac{dr}{r^2} W_{\chi 2}(r) W_g(r) P_{\rho^2} \left(k = \frac{l}{r}, z(r) \right). \quad (24)$$

As a simplifying hypothesis we again neglect the matter-galaxy bias. Notice further that in a galaxy catalogue galaxies are observed directly so that the ρ_g from the catalogue already contains the redshift evolution and no further $(1+z)^3$ factors are needed. The function $W_g(z) = dn/dz(z)$ is characteristic of the survey and of its depth i.e. the mean observed redshift. In the following we will assume the typical shape

$$W_g(z) = \frac{dn}{dz}(z) = (z - z_c)^2 \exp \left[- \left(\frac{z - z_c}{z_0 - z_c} \right)^{1.5} \right], \quad (25)$$

where z_0 is the mean redshift depth of the survey and z_c is the low z cutoff. For definiteness we will consider a 2MASS-like catalogue with $z_0 = 0.1$ and $z_c = 0$.

The error bars for these observables are this time given by a more involved expression

$$\frac{\delta C_{\gamma g}^l}{C_{\gamma g}^l} = \sqrt{\frac{1}{(2l+1)\Delta l f_{\text{fov}}} \left(1 + \frac{C_\gamma^l C_g^l}{C_{\gamma g}^l C_{\gamma g}^l} (1 + C_{N,\gamma}/W_l^2 C_\gamma^l)(1 + C_{N,g}/W_l^2 C_g^l) \right)}, \quad (26)$$

$$\frac{\delta C_{\chi g}^l}{C_{\chi g}^l} = \sqrt{\frac{1}{(2l+1)\Delta l f_{\text{fov}}} \left(1 + \frac{C_\chi^l C_g^l}{C_{\chi g}^l C_{\chi g}^l} (1 + C_{N,\chi}/W_l^2 C_\chi^l)(1 + C_{N,g}/W_l^2 C_g^l) \right)}, \quad (27)$$

where $C_{N,g} = \Omega_{\text{fov}}/N_g$ is the galaxy random noise, analogous to $C_{N,\gamma}$ and $C_{N,\chi}$, where N_g is the number of galaxies in the survey. For the case of the 2MASS survey we assume $f_{\text{sky}} \simeq 0.8$ and $N_g \simeq 10^6$. We have further assumed that the CGB and galaxy maps have been smoothed to the same angular resolution so that the same W_l can be used. The use of cross-correlation with galaxies has been proven to be a powerful tool in cosmology, in particular in the analysis of the Cosmic Microwave Background Radiation [38, 39]. A cross-correlation with galaxies has also been suggested in the study of the MeV gamma background [40]. We refer the reader to these references for further details on the formalism employed.

The results are shown in Fig. 5 with the same assumptions as in Fig. 4 for N_γ and N_χ . It can be seen that in general the galaxy-CGB spectrum is less optimal with respect to the auto-correlation spectrum of the CGB itself to look for differences between DM and astrophysical sources, but there are still some discerning power. The same trend as in Fig. 4 is recognizable: At $E_{\text{cut}} = 100$ GeV the fluctuations in the DM spectrum are higher with respect to the astrophysical case and the statistics and angular resolution expected from GLAST can distinguish the two cases. At $E_{\text{cut}} = 100$ GeV the balance between enhanced DM fluctuations and horizon dilution makes degenerate the normalization of the two contributions. However, the different shapes at $l \gtrsim 100$ still allow to disentangle the two cases. Notice that in all cases the intermediate scale multipoles $l \sim 100$ appear to be optimal to disentangle the two cases.

Although in the single case shown the cross-correlation appears to be less sensitive to DM signatures compared to the auto-correlation of the CGB, it has to be stressed that this is an independent observable and the two can be combined and used at the same time improving the statistical power of the analysis. Further, different catalogues can be employed with, possibly, a more suitable window that can enhance the sensitivity of the cross-correlation. Finally, if the catalogue is sufficiently deep (like for example the case of the SDSS main sample and the high redshift Luminous Red Galaxies sample [39]) it can be possible to split the galaxy distribution into various redshift bins and perform a tomography analysis with different independent cross-correlations.

VI. CROSS-CORRELATION BETWEEN ENERGY BANDS

The cross-correlation formalism introduced in the previous section can be further employed in comparing the CGB anisotropies in *different energy bands*. In particular, at the low energy band $E \lesssim 1 - 10$ GeV the DM contribution is expected to be negligible. This energy range thus represents a natural, high statistics template of the astrophysical gamma sky to compare with for the higher, $E \gtrsim 10$ GeV, DM relevant energy bands considered above.

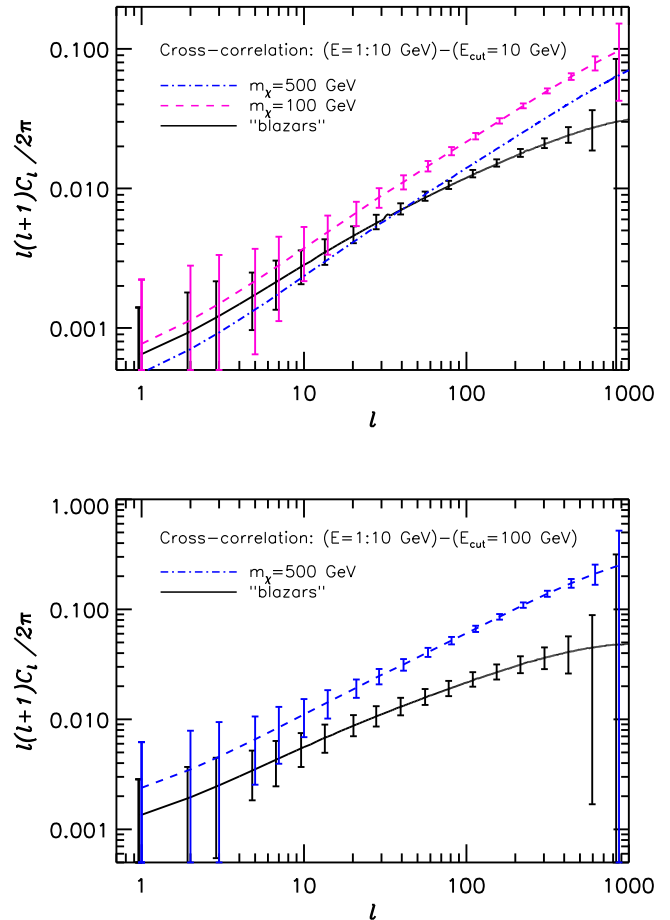


FIG. 6: Cross-correlation between the energy bands $E = 1:10$ GeV ($1 \text{ GeV} < E < 10 \text{ GeV}$), where the DM contribution is assumed to be negligible, and $E_{\text{cut}} = 10, 100$ GeV. The errors refer to a 4-year GLAST survey.

As an example we plot in Fig. 6 the cross-correlation between the energy bands $E = 1 : 10$ GeV (i.e. $1 \text{ GeV} < E < 10 \text{ GeV}$), where the DM contribution is assumed to be negligible, and $E_{\text{cut}} = 10, 100$ GeV as for Figs. 4 and 5 for an astrophysical dominated CGB and for a DM dominated CGB for various WIMP masses m_χ . It can be seen that the diagnostic power is similar to that of the auto-correlation of Fig. 4, understandable in the light of the close similarity between the $E_{\text{cut}} = 10, 100$ GeV CGB and the template we are comparing with. The cross-correlation between different energy bands thus represents a further independent observable sensitive to DM signatures. In particular, it acts complementary to the auto-correlation spectrum, providing an effective, high statistics, calibration of the astrophysical background at low energy, thus allowing more easily to distinguish the sought DM signal at higher energies.

VII. DISCUSSION

A. Mixed scenario

We have seen that a particularly clear signature of DM annihilation in the CGB is present in our “quadratic scenario”. However, a certain contribution from sub-galactic clumps and thus a mixing of the linear and quadratic scenarios is anyway expected, although, as previously discussed, the relative contribution is still quite uncertain. A contribution to the DM signal from sub-galactic clumps is particularly interesting due to the fact that it is expected to enhance the overall DM annihilation signal of roughly one order of magnitude increasing correspondingly the chances of detection [8, 13, 15]. To give a hint of how this contribution affects the previous conclusions we show in Fig. 7 the auto-correlation spectrum of DM for $E_{\text{cut}} = 100$ GeV and for a $m_\chi = 500$ GeV WIMP in the case in which 80% of the DM signal correlate linearly with matter and only 20% of the DM contribution correlate quadratically, the sum being at the level of the EGRET flux. Given that DM in the linear scenario is almost degenerate with a pure astrophysical emission, an equivalent interpretation of Fig. 7 is that of a subdominant, 20% level, quadratic DM contribution, and an overall signal dominated by astrophysical emission. We see that in both cases the prospects are quite interesting and the DM spectrum still differs significantly from that of a background generated by astrophysical sources only.

In the “worst” case, i.e. our “linear scenario”, in which sub-galactic clumps dominate the annihilation signal, the anisotropies are degenerate with the astrophysical signal and the signature in the CGB disappear. In second approximation some difference is still expected due to the presence of a bias in the relative distributions of DM and astrophysical sources, although the signature become quite model dependent (see [22] for a more detailed discussion). However, in this case, unless our galaxy is unrepresentative of an average galactic halo, the best chances to detect the DM gamma signal, clearly, would come from the Milky Way halo itself for which other kinds of anisotropy signatures, due basically to the peculiar profile of the galactic halo, are expected (see for example [12, 29] for more details). In this respect, it is interesting to notice this sort of complementarity between DM signatures in the extragalactic cosmological signal and the local galactic signal.

B. CGB normalization

Part of the population of sources contributing to the CGB will likely be resolved by GLAST consequently lowering the level of unresolved emission and thus the intensity of the CGB. This, indeed, will turn out as an advantage given that only astrophysical sources are resolved and thus the signal to noise ratio for DM is *enhanced*. An estimate in the framework of the blazar model of the

CGB of [41] suggests that GLAST could lower the CGB by a factor of 2 [8]. As an extreme assumption we plot in Fig. 8 the error bars in the case in which the CGB (and thus the statistics) is reduced by a factor of 5 (i.e. to 20% of the present value), assuming the pure quadratic DM scenario. We see that even in this case the statistics are good enough to separate the two angular spectra. Notice that the result is quite conservative given that in the figure both the CGB and the DM signal are reduced by a factor of 5.

Although not shown, a very similar result applies for the case of a cross-correlation between different CGB energy bands that thus equally maintain its diagnostic power in a low statistics regime. The sensitivity of the galaxies-CGB cross-correlation is instead sensibly reduced both in the low and the high energy ranges. Finally, if we consider the mixed scenario in the framework of this low statistics CGB then the prospects of DM detection became quite low. A 20% DM quadratic contribution in this case would correspond to a 4% contribution with respect to the present EGRET intensity, making the anisotropy transition signature quite challenging to detect.

C. Foreground removal

Finally, we comment on the role of the galactic foreground on the results. The foreground subtraction remains a delicate issue, as can be appreciated by the reanalysis of the EGRET data performed in [42], based on a revised model for the galactic propagation of cosmic rays that resulted in an appreciably different spectral behavior compared to Eq. (16) and in a slight change in the overall normalization. The foreground subtraction is also expected to alter and enlarge in a non-trivial way the estimate in Eqs. (19-20) of the error bars of the angular spectrum. A detailed estimate of this effect is beyond the scope of the present work. Possibly, however, the effect of galactic contamination can be kept under control enlarging the galactic cut to higher galactic latitudes $b \gtrsim 20^\circ$ where the galactic emission is expected to rapidly decrease [36, 42], although at the price of reducing correspondingly the available statistics. Residual foregrounds are anyway expected even at the highest latitudes, at a level depending on the foreground model used, making non-obvious also this simple first order analysis. An accurate analysis, further, should eventually rely on a full simulation of the data analysis pipeline.

Further, if, as considered above, clumpiness in the Milky Way halo becomes relevant, then, in principle, the resulting DM annihilation signal has to be considered as a further galactic foreground. CGB extraction, in this case, would become more challenging due to the need to include in consistent way DM annihilation both in the galactic and the extra-galactic signal (see, indeed, ref. [27] where an iterative procedure is applied both to the galactic foreground and the extra-galactic back-

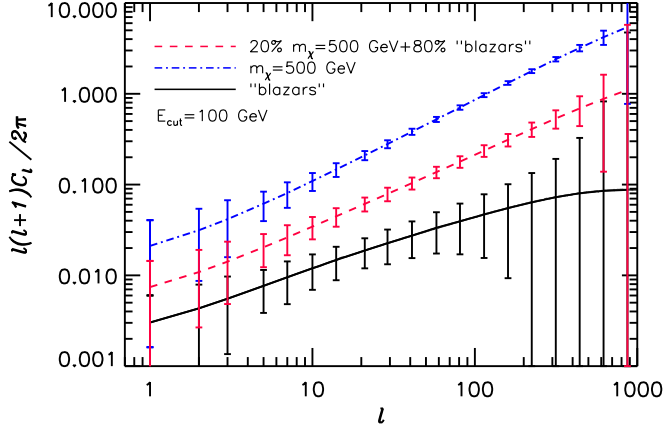


FIG. 7: Angular spectra for $E_{\text{cut}} = 100$ GeV. Shown are the cases of CGB dominated by “blazars”, CGB dominated by a $m_\chi = 500$ GeV WIMP and CGB contributed by a $m_\chi = 500$ GeV WIMP for 20% and by “blazars” for 80%. This latter case is degenerate with a CGB contributed entirely by DM with a 20% emission tracing the matter quadratically and an 80% emission tracing the matter linearly. The errors refer to the statistics expected from a 4-year GLAST survey.

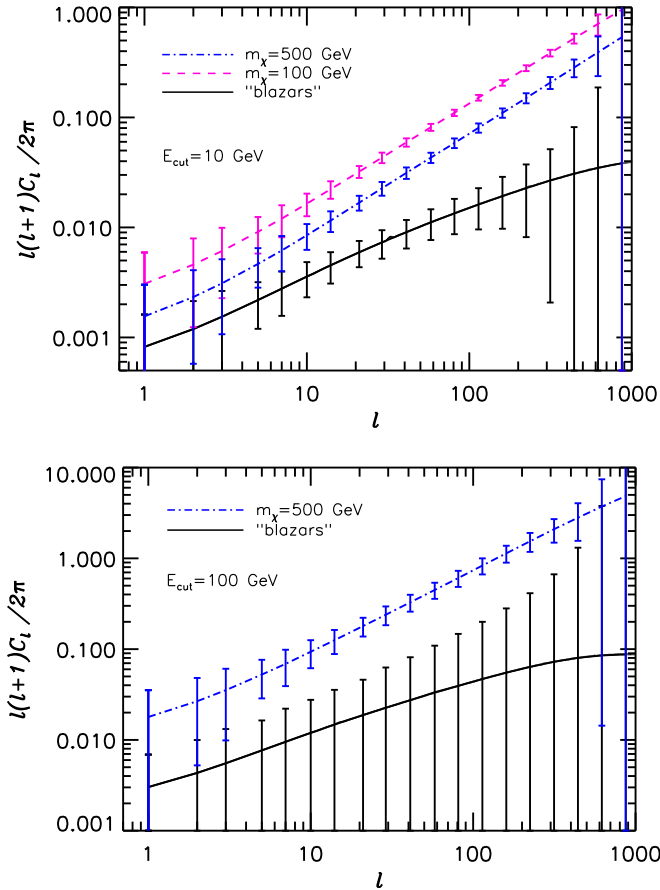


FIG. 8: As in Fig. 4, but for a DM and astrophysical signal 5 times lower (i.e 20% of the present EGRET value).

ground for the claim of DM detection in the EGRET

data).

VIII. SUMMARY AND CONCLUSIONS

In the present work we have studied the kind of signatures that DM annihilation is expected to imprint in the anisotropies of the CGB, complementary to the signatures in the energy spectrum. We have addressed the main physical ingredients contributing to the DM signature and discussed the robustness of the signature with respect to various possible scenarios. We can summarize our findings as follows:

- The DM annihilation signal traces in general the matter distribution quadratically due to its ρ_χ^2 dependence. However, an effective linear correlation can arise if the signal is significantly enhanced by the presence of cuspy haloes or sub-galactic clumps. We have defined the two extreme “linear” and “quadratic” scenarios. The first corresponds to the case in which the cosmological DM annihilation signal is dominated by galactic or sub-galactic structures while in the second the signal is dominated by emission on scales larger than that of a galactic halo. We have chosen a phenomenological approach introducing a parameter ξ that weights the two relative contributions exploring the DM signatures for different possible choices of ξ .
- The anisotropies are determined both by the intrinsic fluctuations in the source field and by the size of the emission horizon z_H . For $E_{\text{cut}} \gtrsim 100$ GeV the horizon z_H is essentially fixed by photon absorption in the EBL. The bulk of the gamma-rays is expected to originate inside $z_H \approx 0.5$, independent of whether they have a DM or an astrophysical origin. For $E_{\text{cut}} \gtrsim 10$ GeV, DM annihilation in the quadratic scenario has a redshift horizon $z_H \approx 3 - 4$. The horizon is still significantly limited by PP losses at this energy, otherwise exceeding $z_H \approx 10$. Blazars and DM in the linear scenario have degenerate horizons $z_H \approx 1$.
- In the quadratic scenario the DM anisotropy signal is sensibly enhanced with respect to blazars for $E_{\text{cut}} = 10$ GeV. Further, also the shapes of the angular spectra differ significantly [20, 22]. The signature remain standing also for $E_{\text{cut}} = 100$ GeV despite the decreased statistics and become particularly strong, being independent of uncertainties related to the blazar-matter bias or to the evolution of blazars. This scenario can easily be detected by GLAST and would constitute a strong signature of DM annihilation. The DM linear scenario, instead, exhibit the same level of fluctuations of blazars and the two thus have almost degenerate anisotropy features.

- The above signature in the angular spectrum remains quite robust as long as the quadratic DM signal is at least at the 10-20% level with respect to the linear DM or the blazar component. A further uncertainty to take into account is the normalization of the CGB (and thus the available statistics) that is likely to be reduced if part of the sources contributing to the CGB will be resolved by GLAST. If the normalization is reduced by an extreme factor of 5, (20% of the present EGRET value), the pure quadratic DM scenario exhibits still a relevant anisotropy transition signature. If the quadratic DM contributes for a 20% (thus, 4% of the present EGRET value) then the detection of the signature becomes quite challenging.
- The cross-correlation between the CGB and a survey of galaxies and the cross-correlation between different energy bands of the CGB provide further independent and sensitive observables that can be employed in combination with the CGB auto-correlation. A joint analysis of all the anisotropy observables considerably improves the sensitivity to the DM signal and, more in general, the power of the statistical analysis. In principle, the exact contribution from DM annihilation in sub-galactic clumps and cuspy haloes can be treated as free parameters (instead of relying on a model) and inferred from the analysis.

The above conclusions hold exactly if a perfect cleaning of the galactic foregrounds and a lossless extraction of the CGB signal is possible. The analysis of foregrounds

will be likely the main challenge in the study of the CGB. Clearly, given the above shown potential of CGB anisotropies in looking for DM signatures, it would be worth to perform further detailed studies on the issue. The launch of the GLAST satellite is expected by the middle of 2008, while the satellite AGILE [43] launched in April 2007 is currently already taking data. The improvement in statistics compared to EGRET will allow for new, powerful tools to search for exotic contributions to the gamma-ray signal. The anisotropy analysis of the CGB in particular, if foregrounds contaminations can be efficiently kept under control, promises to provide a clear signature of DM annihilation or, in the case of a negative answer, to obtain new constraints on the DM properties, complementary to a pure energy spectrum analysis.

Acknowledgments

The authors wish to thank P. D. Serpico for fruitful discussions and for valuable comments on the manuscript. H. Tu is kindly acknowledged for providing us the Halo-model power spectrum. We thank the Danish Centre of Scientific Computing (DCSC) for granting the computer resources used. TH acknowledges partial financial support from the Spanish Research Ministry (MEC), under the contract FPA2006-05807. GM acknowledges supports by Generalitat Valenciana (ref. AINV/2007/080 CSIC) and by PRIN 2006 "Fisica Astroparticellare: neutrini ed universo primordiale" by the Italian MIUR.

-
- [1] G. Bertone, D. Hooper and J. Silk, "Particle dark matter: Evidence, candidates and constraints," *Phys. Rept.* **405**, 279 (2005) [arXiv:hep-ph/0404175].
 - [2] M. Tegmark *et al.*, "Cosmological Constraints from the SDSS Luminous Red Galaxies," *Phys. Rev. D* **74**, 123507 (2006) [arXiv:astro-ph/0608632].
 - [3] D. N. Spergel *et al.* [WMAP Collaboration], "Wilkinson Microwave Anisotropy Probe (WMAP) three year results: Implications for cosmology," *Astrophys. J. Suppl.* **170**, 377 (2007) [arXiv:astro-ph/0603449].
 - [4] U. Seljak, A. Slosar and P. McDonald, "Cosmological parameters from combining the Lyman-alpha forest with CMB, galaxy clustering and SN constraints," *JCAP* **0610**, 014 (2006) [arXiv:astro-ph/0604335].
 - [5] J. Hamann, S. Hannestad, M. S. Sloth and Y. Y. Y. Wong, "How robust are inflation model and dark matter constraints from cosmological data?," *Phys. Rev. D* **75**, 023522 (2007) [arXiv:astro-ph/0611582].
 - [6] K. Griest and M. Kamionkowski, "Unitarity Limits on the Mass and Radius of Dark Matter Particles," *Phys. Rev. Lett.* **64**, 615 (1990).
 - [7] J. F. Gunion, D. Hooper and B. McElrath, "Light neutralino dark matter in the NMSSM," *Phys. Rev. D* **73** (2006) 015011 [arXiv:hep-ph/0509024].
 - [8] P. Ullio, L. Bergstrom, J. Edsjo and C. G. Lacey, "Cosmological dark matter annihilations into gamma-rays: A closer look," *Phys. Rev. D* **66**, 123502 (2002) [arXiv:astro-ph/0207125].
 - [9] L. Bergstrom, J. Edsjo and P. Ullio, "Spectral gamma-ray signatures of cosmological dark matter annihilations," *Phys. Rev. Lett.* **87**, 251301 (2001) [astro-ph/0105048].
 - [10] D. Elsaesser and K. Mannheim, "Supersymmetric dark matter and the extragalactic gamma ray background," *Phys. Rev. Lett.* **94** (2005) 171302 [arXiv:astro-ph/0405235].
 - [11] D. Elsaesser and K. Mannheim, "Cosmological gamma ray and neutrino backgrounds due to neutralino dark matter annihilation," *Astropart. Phys.* **22** (2004) 65 [arXiv:astro-ph/0405347].
 - [12] L. Pieri, G. Bertone and E. Branchini, "Dark Matter Annihilation in Substructures Revised," arXiv:0706.2101 [astro-ph].
 - [13] J. E. Taylor and J. Silk, "The clumpiness of cold dark matter: Implications for the annihilation signal," *Mon. Not. Roy. Astron. Soc.* **339** (2003) 505 [arXiv:astro-ph/0207299].
 - [14] V. Berezhinsky, V. Dokuchaev and Y. Eroshenko, "Destruction of small-scale dark matter clumps in the hier-

- archical structures and galaxies,” *Phys. Rev. D* **73** (2006) 063504 [arXiv:astro-ph/0511494].
- [15] L. Bergstrom, J. Edsjo, P. Gondolo and P. Ullio, “Clumpy neutralino dark matter,” *Phys. Rev. D* **59** (1999) 043506 [arXiv:astro-ph/9806072].
- [16] J. Diemand, M. Kuhlen and P. Madau, “Dark matter substructure and gamma-ray annihilation in the Milky Way halo,” *Astrophys. J.* **657** (2007) 262 [arXiv:astro-ph/0611370].
- [17] J. Diemand, B. Moore and J. Stadel, “Earth-mass dark-matter haloes as the first structures in the early universe,” *Nature* **433** (2005) 389 [arXiv:astro-ph/0501589].
- [18] E. A. Baltz, J. E. Taylor and L. L. Wai, “Can Astrophysical Gamma Ray Sources Mimic Dark Matter Annihilation in Galactic Satellites?,” arXiv:astro-ph/0610731.
- [19] A. Cuoco, S. Hannestad, T. Haugbolle, G. Miele, P. D. Serpico and H. Tu, “The Signature of Large Scale Structures on the Very High Energy Gamma-Ray Sky,” *JCAP* **0704** (2007) 013 [arXiv:astro-ph/0612559].
- [20] S. Ando and E. Komatsu, “Anisotropy of the cosmic gamma-ray background from dark matter annihilation,” *Phys. Rev. D* **73**, 023521 (2006) [astro-ph/0512217].
- [21] S. Ando, E. Komatsu, T. Narumoto and T. Totani, “Angular power spectrum of gamma-ray sources for GLAST: blazars and clusters of galaxies,” *Mon. Not. Roy. Astron. Soc.* **376** (2007) 1635 [arXiv:astro-ph/0610155].
- [22] S. Ando, E. Komatsu, T. Narumoto and T. Totani, “Dark matter annihilation or unresolved astrophysical sources? Anisotropy probe of the origin of cosmic gamma-ray background,” *Phys. Rev. D* **75** (2007) 063519 [arXiv:astro-ph/0612467].
- [23] F. Miniati, S. M. Koushiappas and T. Di Matteo, “Angular Anisotropies in the Cosmic Gamma-ray Background as a Probe of its Origin,” arXiv:astro-ph/0702083.
- [24] W. de Boer, C. Sander, V. Zhukov, A. V. Gladyshev and D. I. Kazakov, “EGRET excess of diffuse galactic gamma rays as tracer of dark matter,” *Astron. Astrophys.* **444** (2005) 51 [arXiv:astro-ph/0508617].
- [25] L. Bergstrom, J. Edsjo, M. Gustafsson and P. Salati, “Is the dark matter interpretation of the EGRET gamma excess compatible with antiproton measurements?,” *JCAP* **0605** (2006) 006 [arXiv:astro-ph/0602632].
- [26] W. de Boer, I. Gebauer, C. Sander, M. Weber and V. Zhukov, “Is the dark matter interpretation of the EGRET gamma ray excess compatible with antiproton measurements?,” *AIP Conf. Proc.* **903** (2007) 607 [arXiv:astro-ph/0612462].
- [27] W. de Boer, A. Nordt, C. Sander and V. Zhukov, “A new Determination of the Extragalactic Background of Diffuse Gamma Rays taking into account Dark Matter Annihilation,” *Astron. Astrophys.* **470** (2007) 61, arXiv:0705.0094 [astro-ph].
- [28] F. W. Stecker, M. A. Malkan and S. T. Scully, “Intergalactic photon spectra from the far IR to the UV Lyman limit for $0 < z < 6$ and the optical depth of the universe to high energy gamma-rays,” *Astrophys. J.* **648**, 774 (2006) [astro-ph/0510449]. See also F. W. Stecker, M. A. Malkan and S. T. Scully, “Corrected Table for the Parametric Coefficients for the Optical Depth of the Universe to Gamma-rays at Various Redshifts,” *Astrophys. J.* **658** (2007) 1392 [arXiv:astro-ph/0612048].
- [29] D. Hooper and P. D. Serpico, “Angular Signatures of Dark Matter in the Diffuse Gamma Ray Spectrum,” *JCAP* **0706** (2007) 013 [arXiv:astro-ph/0702328].
- [30] V. Springel, “The cosmological simulation code GADGET-2,” *Mon. Not. Roy. Astron. Soc.* **364** (2005) 1105 [arXiv:astro-ph/0505010].
- [31] U. Seljak and M. Zaldarriaga, “A line of sight approach to cosmic microwave background anisotropies,” *Astrophys. J.* **469** (1996) 437 [astro-ph/9603033].
- [32] M. Crocce, S. Pueblas and R. Scoccimarro, “Transients from Initial Conditions in Cosmological Simulations,” astro-ph/0606505.
- [33] Monaghan, J.J. and Lattanzio, J.C., *Astron. Astrophys.* **149** (1985) 135.
- [34] A. Jenkins *et al.* [Virgo Consortium Collaboration], “Evolution of structure in cold dark matter universes,” *Astrophys. J.* **499** (1998) 20 [arXiv:astro-ph/9709010].
- [35] R. E. Smith *et al.* [The Virgo Consortium Collaboration], “Stable clustering, the halo model and nonlinear cosmological power spectra,” *Mon. Not. Roy. Astron. Soc.* **341** (2003) 1311 [astro-ph/0207664].
- [36] P. Sreekumar *et al.* [EGRET Collaboration], “EGRET observations of the extragalactic gamma ray emission,” *Astrophys. J.* **494**, 523 (1998) [astro-ph/9709257].
- [37] See the URL: <http://www-glast.slac.stanford.edu/>
- [38] N. Afshordi, Y. S. Loh and M. A. Strauss, “Cross-Correlation of the Cosmic Microwave Background with the 2MASS Galaxy Survey: Signatures of Dark Energy, Hot Gas, and Point Sources,” *Phys. Rev. D* **69** (2004) 083524 [arXiv:astro-ph/0308260].
- [39] A. Cabre, E. Gaztanaga, M. Manera, P. Fosalba and F. Castander, “Cross-correlation of WMAP 3rd year and the SDSS DR4 galaxy survey: new evidence for Dark Energy,” *Mon. Not. Roy. Astron. Soc. Lett.* **372** (2006) L23 [arXiv:astro-ph/0603690].
- [40] P. J. Zhang and J. F. Beacom, “Angular Correlations of the MeV Cosmic Gamma Ray Background,” *Astrophys. J.* **614** (2004) 37 [arXiv:astro-ph/0401351].
- [41] F. W. Stecker and M. H. Salamon, “The Gamma-Ray Background from Blazars: A New Look,” *Astrophys. J.* **464** (1996) 600 [arXiv:astro-ph/9601120].
- [42] A. W. Strong, I. V. Moskalenko and O. Reimer, “A new determination of the extragalactic diffuse gamma-ray background from EGRET data,” *Astrophys. J.* **613**, 956 (2004) [astro-ph/0405441].
- [43] See the URL: <http://agile.rm.iasf.cnr.it/>